

An object based image analysis approach to testing the effect of flowering and patch size on *Limonium ramosissimum* detection using CIR and IKONOS imagery

Abstract:

Remote sensing is a useful tool to detect and map invasive plants, but detection success depends on the spectral properties of individual species, their context, and the imagery used for mapping. Using an object based image analysis (OBIA) approach as well as pairwise correlations and pixel-based unsupervised classifications, the efficacy of two different image sources, 30 cm aerial color infrared imagery and 1 m pan-sharpened multispectral IKONOS satellite imagery, were tested to detect an invasive forb, *Limonium ramosissimum ssp provinciale* during its peak flowering period in salt marshes where it has been previously mapped with GPS. Using a variety of spectral layers, indices, rule sets, and unsupervised classifications parameters, regardless of the patch size, the degree to which patches were in flower at the time of image acquisition, or the imagery source, the invasive was not distinguishable from surrounding high marsh and transitional upland habitat. To integrate remote sensing into a comprehensive weed management program, a systematic review of which invasive species can be detected at what scale by which sources of imagery is recommended.

Introduction:

Invasive plant species are a major management concern in wetland ecosystems. In the San Francisco Bay estuary, a number of non-native salt tolerant plant species have emerged as a priority for land managers (Grossinger et al, 1998). Monitoring these invasions and detecting new ones, such as priority species recently identified by the Bay Area Early Detection Network (www.baedn.org, 2010) remains a priority and challenge for land managers.

Remote sensing offers a unique tool to identify invasive plants (Lass et al, 2005), particularly in large wilderness areas where ground mapping can be difficult and time consuming, and in sensitive habitats like wetlands. But the ability to detect invasive plants varies by species, and by the scale of interest. For example, invasive hybrid *Spartina* patches in San Francisco Bay marshes are readily mapped via manual interpretation and digitization of aerial imagery in cases when hybrid *Spartina* grows significantly more vigorously than the native, but remote sensing is not possible when hybrid patches are morphologically similar to natives, covered by dead standing vegetation, and when patches are smaller than the imagery resolution (Hogle, personal communication, 2010).

Another high impact invasive in San Francisco Bay marshes, *Lepidium latifolium*, is readily mapped with hyperspectral imagery (Andrew and Ustin, 2006) and multispectral satellite imagery (Fulfrust, personal communication, 2010), though the minimum detectable patch size likely varies between imagery sources, a consideration relevant if a goal of mapping is early detection of new populations.

In 2007, a non-native salt tolerant plant which invades marshes in Southern California, *Limonium ramosissimum ssp provinciale*, was found at a restored marsh in South San Francisco Bay. There, GPS mapping revealed it has heavily recruited in the footprint of a 1987 marsh restoration project (Archbald and Boyer, 2010). Since then populations have been found and mapped with GPS at 20 restored and historic tidal salt marshes in the Bay. The plant establishes primarily in the high marsh and grows in dense patches, particularly along the upland transition boundary (Archbald and Boyer, 2010), a habitat utilized by 4 of the 6 plant

and vertebrate species listed as rare or endangered in the Bay (Josselyn, 1983). This plant was recently included in the Bay Area Early Detection Network's Priority Species List for identification and removal (BAEDN, 2010).

In 2009, a project funded by the South Bay Salt Pond (SBSP) Restoration Project was initiated to map *L. ramosissimum* in marshes in and around the 15,000 acre Project area. One of the goals of the SBSP project is to maximize native marsh habitat and minimizing invasive plants in restored marshes, and locations of *L. ramosissimum* populations (Figure 1, Appendix) suggest the plant is likely to impact restored high marsh habitat if left unmanaged. To search for additional populations, a species distribution model for was developed and used to guide boat and ground based searches for the plant. These searches identified populations, but finding and mapping *L. ramosissimum* populations in marshes that have not been searched, and monitoring populations into the future would be facilitated by a more comprehensive detection approach using remote sensing.

Many invasive species have been successfully mapped with aerial and satellite imagery (see Lass, et al 2005 for a review). In general, species are easiest to detect when they are spectrally distinct from the surrounding landscape, and therefore many mapping studies make use of seasonal phenology and map during times of greatest spectral variability, such as when species are in flower (Cuneo, 2009; Everitt et al 1996; Hunt et al, 2010; Lass and Prather, 2004). *L. ramosissimum* has distinctive, showy, abundant purple and white flowers (Figure 1), and blooms earlier than the native *L. californicum*, a trait which may help differentiate the invasive from surrounding vegetation via remote sensing.



Figure 1: Invasive *L. ramosissimum* in flower at Coyote Point Marina in S. San Francisco Bay.

Mapping and detection is also most readily accomplished with remote sensing when species occur in patches larger than the spatial resolution of the imagery (Rosso, Ustin and Hastings, 2005), yet early detection and rapid response, the most cost effective method for dealing

with invasive species (Westbrooks, 2004), depends on identifying populations when they are small. Because of this, high spatial resolution imagery is required for early detection, though even the highest resolution imagery source will have a minimum detectable patch size which must be experimentally determined, and which will vary by the species, and the context that species occurs in.

Different imagery sources have proven to be of different utility in species mapping. One mapping study, for example, found that an invasive plant, leafy spurge, could be detected with hyperspectral satellite imagery, but not with multispectral satellite imagery (Hunt and Williams, 2006). Interestingly, the reason for this difference was concluded to be because more sophisticated classification algorithms are available for hyperspectral imagery, rather than a function of the spectral signature of the plant relative to the range of the multispectral sensor used for imagery acquisition.

However, hyperspectral imagery does not always offer an advantage in species detection. A mapping study of tidal salt marsh plants, which included a *Limonium* species, compared a range of satellite and aerial imagery sources and found no advantage to using hyperspectral relative to multispectral imagery. In fact, mapping accuracy for *Limonium narbonense* was higher for multispectral than hyperspectral imagery and the authors concluded higher spatial resolution was more useful than higher spectral resolution for mapping accuracy (Belluco et al, 2006).

Aerial imagery provides an improvement over satellite imagery in terms of spatial resolution, but is often more expensive to acquire, must be acquired in many more tiles than satellite imagery when mapping at large spatial scales (which introduces variability between images and complicates remote sensing), and often lacks data in the blue range of the spectrum, a loss of spectral resolution that may be significant for detecting some species. Color infrared imagery is frequently used for vegetation mapping because healthy vegetation reflects intensely in the infrared region of the spectrum, and CIR imagery has successfully been used to detect invasive and native marsh species (Tuxen and Kelley, 2008, Lass, et al 2005). While color infrared imagery lacks data in the blue range of the spectrum, its higher resolution versus satellite imagery offers a potential advantage detecting small vegetation patches.

The objectives of this study were to:

1. Determine whether *L. ramosissimum* can be detected with either ~30-cm resolution aerial color infrared imagery or 4-m pan sharpened to 1-m IKONOS multispectral satellite imagery, or both.
2. Determine the degree to which *L. ramosissimum* flowering, percent cover, and patch size influence detection accuracy and how this varies between imagery sources.

Methods:

Study area:

Imagery of two marshes, Coyote Pt Marina and Sanchez Marsh (Figure 2, page 4) were compared for their ability to detect *L. ramosissimum* patches. These marshes were chosen because they have large *L. ramosissimum* populations (Table 1, Appendix) which was

determined by mapping in 2008 (Archbald and Boyer, unpublished) and these populations include large and small patches with high percent cover.

Within days of imagery acquisition, *L. ramosissimum* populations were re-mapped at both sites using a handheld Trimble GeoXH GPS with approximately 30 cm horizontal accuracy. Patches larger than 1 m² were mapped as polygons and smaller patches were mapped as points. Percent cover of *L. ramosissimum* and percent of inflorescences in flower were recorded. Plants greater than 1 m apart were mapped as separate patches. Coyote Point Marina was mapped on 7/8/2010 and Sanchez Marsh on 7/5/2010.

Imagery sources:

Two imagery sources were compared for their ability to detect *L. ramosissimum*- Color infrared aerial imagery with 30 cm pixel resolution and IKONOS 4 m multispectral pan-sharpened to 1 m.



Figure 2: IKONOS satellite and CIR aerial imagery was acquired for (1) Sanchez Creek Marsh and (2) Coyote Point Marina.

Imagery from the IKONOS satellite was acquired by GeoEye on 7/4/2010 (Figure 2, page 5). The IKONOS satellite is equipped with 2 sensors, a .82-meter panchromatic (black and white) a 4 m multispectral sensor (spectral ranges in Table 1, page 5). Images from the 4 m multispectral sensor were pansharpened to 1 m using the panchromatic layer by GeoEye. IKONOS multispectral imagery after pan-sharpening has been used to classify marsh vegetation successfully (Bellusco et al, 2006). The imagery was delivered as a 4-band georeferenced TIFF.

Color infra red aerial imagery was acquired by GeoG2 Solutions on 7/9/2010 (Figure 3, page 5) by airplane at .33m spatial resolution (post-georeferencing). Three monochrome

cameras (Kodak KAF 39000) collected 16-bit images individually filtered at the wavelengths shown in Table 2. Images were delivered as ungeoreferenced TIFFs.

Table 1: Spectral ranges recorded by image sensors and corresponding image bands.

	Individually filtered Kodak KAF 3900 Color infrared (CIR)		IKONOS Multispectral	
Spectral range	Sensor range (nm)	Image band	Sensor range (nm)	Image band
Blue			445-516 nm	1
Green	520-600 nm	Blue	505-595 nm	2
Red	630-690 nm	Green	632-698 nm	3
Near infrared	760-900 nm	Red	757-853 nm	4
Spatial resolution	.33 meter		4 meters pansharpened to 1 meter	

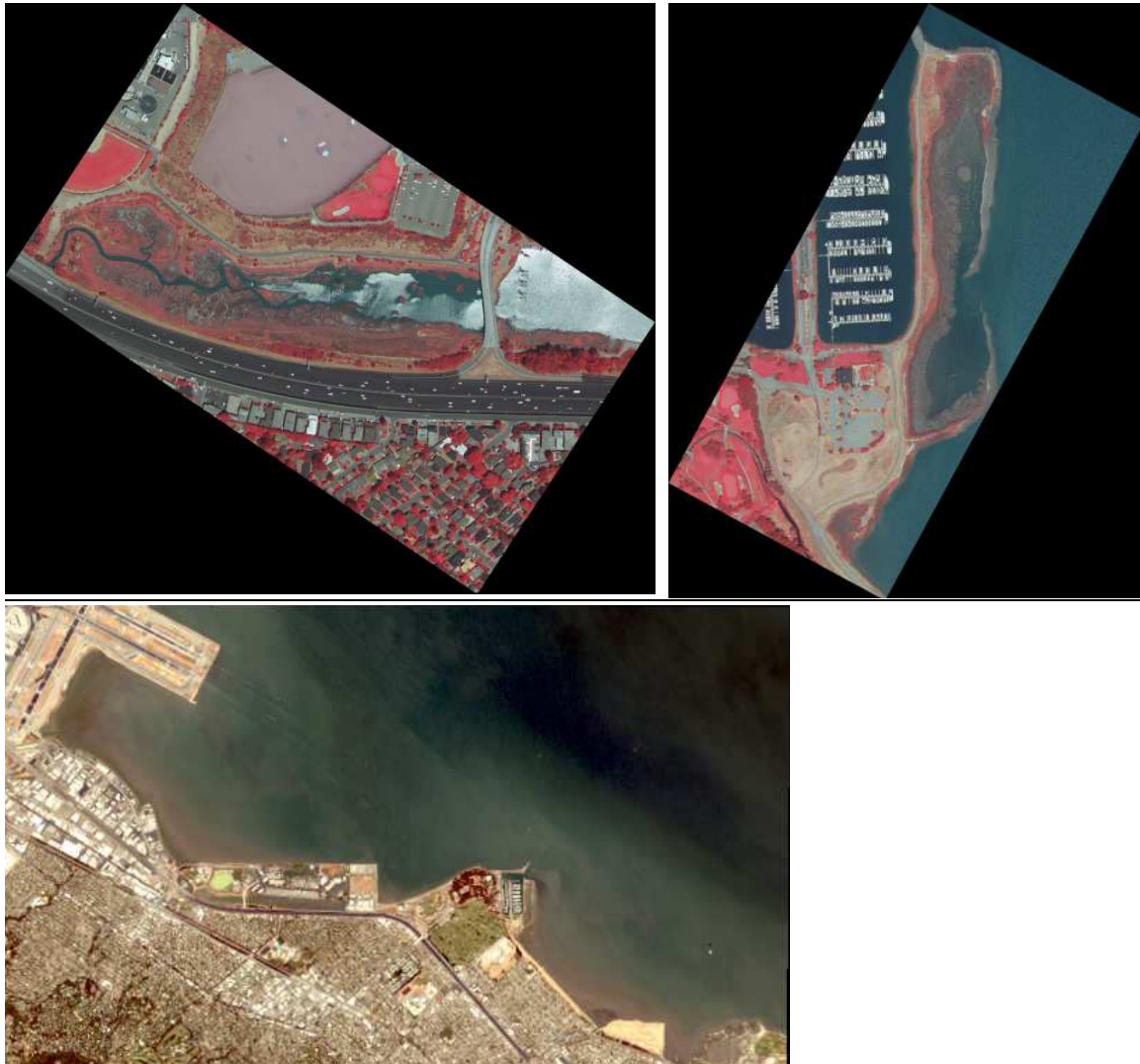


Figure 3: Color infrared imagery for the two study sites were captured as separate tiles (top). Multispectral IKONOS imagery was captured as a single tile (above).

Image Preparation:

CIR aerial imagery was georeferenced using the Georeferencing toolbar in ArcMap 9.3. Control points were set using a combination of the 2004 lidar data set (Foxgrover, 2005), 1 m National Agricultural Information Program 2009 imagery accessed through ESRI's ArcGIS Online service, and ground truthed points collected at time of *L. ramosissimum* mapping in July, 2010. 6-10 control points were established per image and control points were iteratively chosen so that total root mean square error remained less than 1 for each image. Output cell size was determined by using the measuring tool in ArcMap on spatially adjusted images prior to rectification.

The CIR imagery had a slight blurring caused by a shutter glitch on the green filtered camera with the result that the green layer was spatially offset from the other layers. After initial georeferencing, layers were separated and the green layer aligned with the other two using Autosync in Erdas, then layers were restacked for analysis. This correction sharpened the image effectively.

The multispectral IKONOS satellite image, though georeferenced by GeoEye prior to distribution was approximately 5 meters spatially offset at the time of acquisition. To correct this, Coyote Point Marina and Sanchez Creek Marsh subsections were clipped from the image, and each study area was spatially adjusted individually using the Georeferencing toolbar and spatial reference sources listed above.

Images were rectified using the nearest neighbor resampling option. While cubic convolution is recommended for satellite and aerial imagery in ESRI help documentation, the rectification process uses a weighted average from the 16 nearest cells to assign rectified image cell values, which would result in distortion of the spectral values originally assigned to cells at the time of image capture. Nearest neighbor, on the other hand, assigns cell values based on the single nearest cell, which most accurately preserves original cell values (Blesius, personal communication, 2010).

So that individual imagery bands could be evaluated for their ability to detect *L. ramosissimum* alone and in combination, in Erdas Imagine the subset tool was used to separate CIR images at both study sites into the green, red, near infrared layers, and the multispectral imagery at both study sites into the blue, green, red, near infrared layers. Images were converted into 8-bit unsigned .img files for further analysis.

Next, in Erdas, a principle components analysis (PCA) was carried out on the 3-band CIR image, and on the 4-band multispectral image, creating three new data layers for remote sensing analysis per imagery sources at each site: the first, second and third principle components (Figure 4). PCA pulls out the major trends across an image's constituent bands and principle components are often used in the image segmentation step in Definiens Developer (Tuxen and Kelley, 2007) to create objects that identify major habitat trends. A histogram equalization was performed on each principle component, a procedure that helps normalize values across each image.

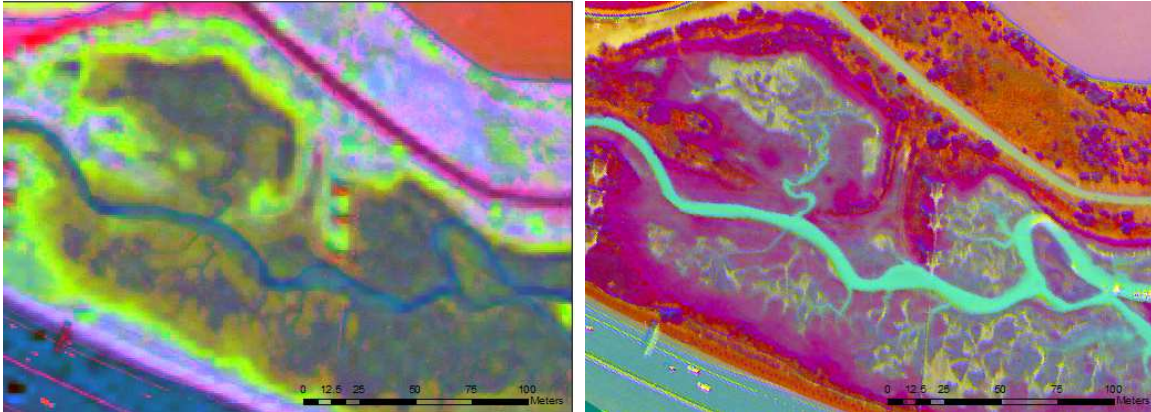


Figure 4: Principle components of the multispectral images (left) and CIR image (right) were recombined into composite images to aid in interpretation and segmentation. The west end of Sanchez Creek Marsh is shown here.

Finally, a Normalized Difference Vegetation Index was created $[(\text{NIR} - \text{red}) / (\text{NIR} + \text{red})]$ using Erdas Modeler for each image at each site. This index, which has widely been used to remotely sense vegetation, measures reflectance in the near-infrared region, which accounts for about 60% of plant reflectance. The index is normalized between -1 and 1 using the red layer, which reduces difference in reflectance across an image resulting from atmospheric conditions (www.csc.noaa.gov, 2010). A histogram equalization was also performed on each NDVI layer, an additional step to normalize reflectance across the images. This index could have been developed in Definiens, as other indices and ratios were, but was carried out in ERDAS so a histogram equalization could also be performed.

The following layers from both imagery sources were then imported into Definiens Developer for both Sanchez Creek Marsh and Coyote Point Marina:

1. Blue layer (multispectral only)
2. Green layer
3. Red layer
4. Near infrared layer
5. First CIR principle component- histogram equalized
6. Second CIR principle component- histogram equalized
7. Third CIR principle component- histogram equalized
8. NDVI layer- histogram equalized

Analysis approach

To test the ability of these imagery sources and layers to detect *L. ramosissimum* in marshes where it has been mapped, an object based image analysis (OBIA) approach using Definiens Developer 7.0 was first used. A rule set was developed using layer, ratio and index values to separate images into broad classes, including high marsh habitat, where *L. ramosissimum* primarily invades. Then, using Definiens, layers, ratios and indices were tested for their ability to further classify habitats with *L. ramosissimum*. This classification approach was carried out at two different spatial scales to test the effect of minimum mapping unit size on detection. Next, Definiens objects with layer, ratio and index values considered most likely to be useful in detecting *L. ramosissimum* were exported and tested for correlation with

percent cover and flowering of *L. ramosissimum* patches. Finally, in Erdas Imagine, unclassified pixel clustering was performed to further test whether spectral properties from either imagery source may be used distinguish *L. ramosissimum* from other species.

Rule set to identify broad habitat classes

In order to classify broad habitat classes, a first step toward isolating *L. ramosissimum* in images, a unique “rule set” was developed through an iterative process for the CIR and multispectral IKONOS imagery (Figures 5 and 6). A rule set includes all the segmentation parameters and classification steps required to convert an image to a meaningful thematic map in Definiens. A unique rule set for each image was necessary because CIR lacks the blue layer useful in classifying the multispectral imagery, and because the same layers and indices varied in their usefulness between imagery sources.

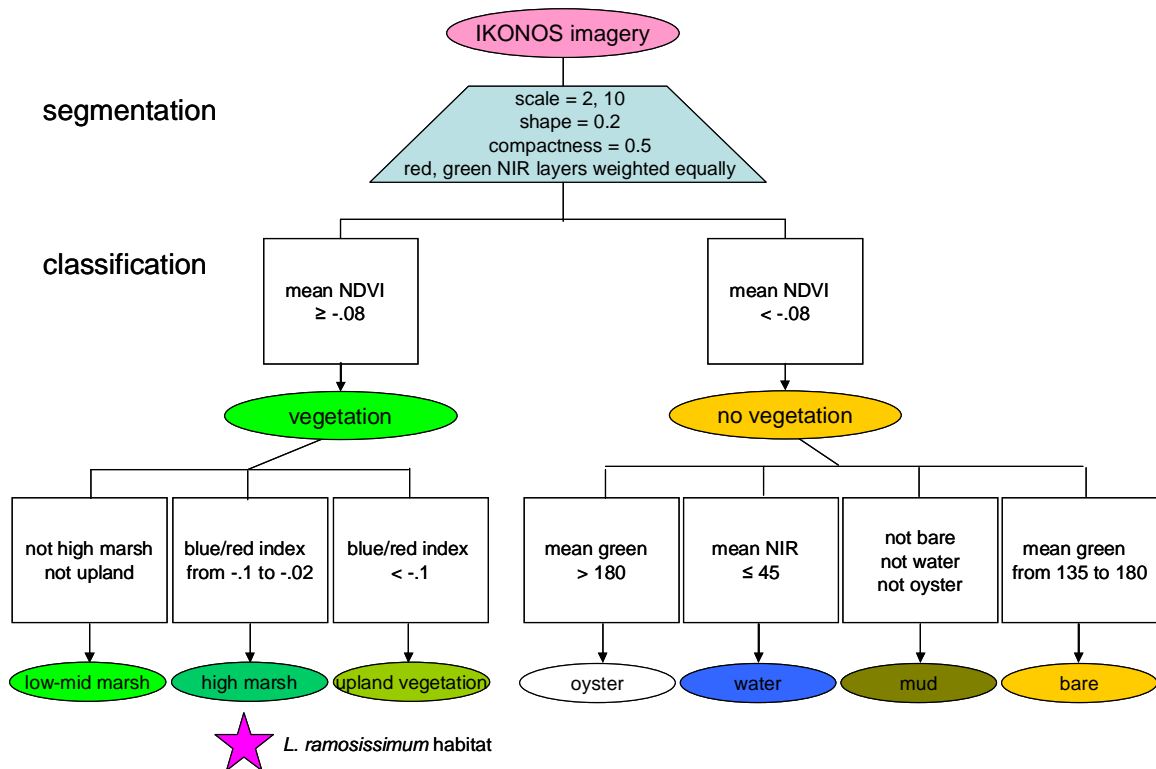


Figure 5: Rule set developed and executed in Definiens Developer 7.0 to identify high marsh habitat and adjacent broad habitat classes using IKONOS imagery. Rule set was run on at two scales: 2 and 10.

Both rule sets were iteratively developed using the northern half of Coyote Point Marina and through a trial and error process. Developing rule sets in Definiens relies on user knowledge of the imagery content, and the north half of Coyote Point Marina was particularly well known, is representative of the major habitat types at both sites, and contains both dense and sparse *L. ramosissimum* patches, and large and small patches in flower. Rule sets were developed through trial and error, but development of indices and ratios guided by previous

studies (ie. Hunt and Williams, 2006; Tuxin and Kelley, 2009). Rule set results were visually checked against the high resolution CIR imagery, as well as against *L. ramosissimum* patch polygons which are known from field mapping to primarily occupy the high marsh, and to a lesser extent the upland border, and bare patches. Also, over 15 visits have been made to both Coytote Point Marina and Sanchez marsh for extensive field work, and a high degree of familiarity with these small marshes helped in imagery interpretation and mapping verification.

The rule sets developed there were then applied to both the southern section of Coyote Point Marina and to Sanchez Creek Marsh for both imagery types. Applying a rule set both within and between images provides a check on the degree to which a rule set's accuracy is a function of within vs. between image variability.

Next, *L. ramosissimum* polygons were used to extract classification results to insure the thematic map effectively limited *L. ramosissimum* locations predominantly to high marsh and upland transition habitat classes. Mapped habitat classes were extracted using in ArcGIS and the relative percent of each habitat classes in ground truthed *L. ramosissimum* polygons were compared by site, scale and image source.

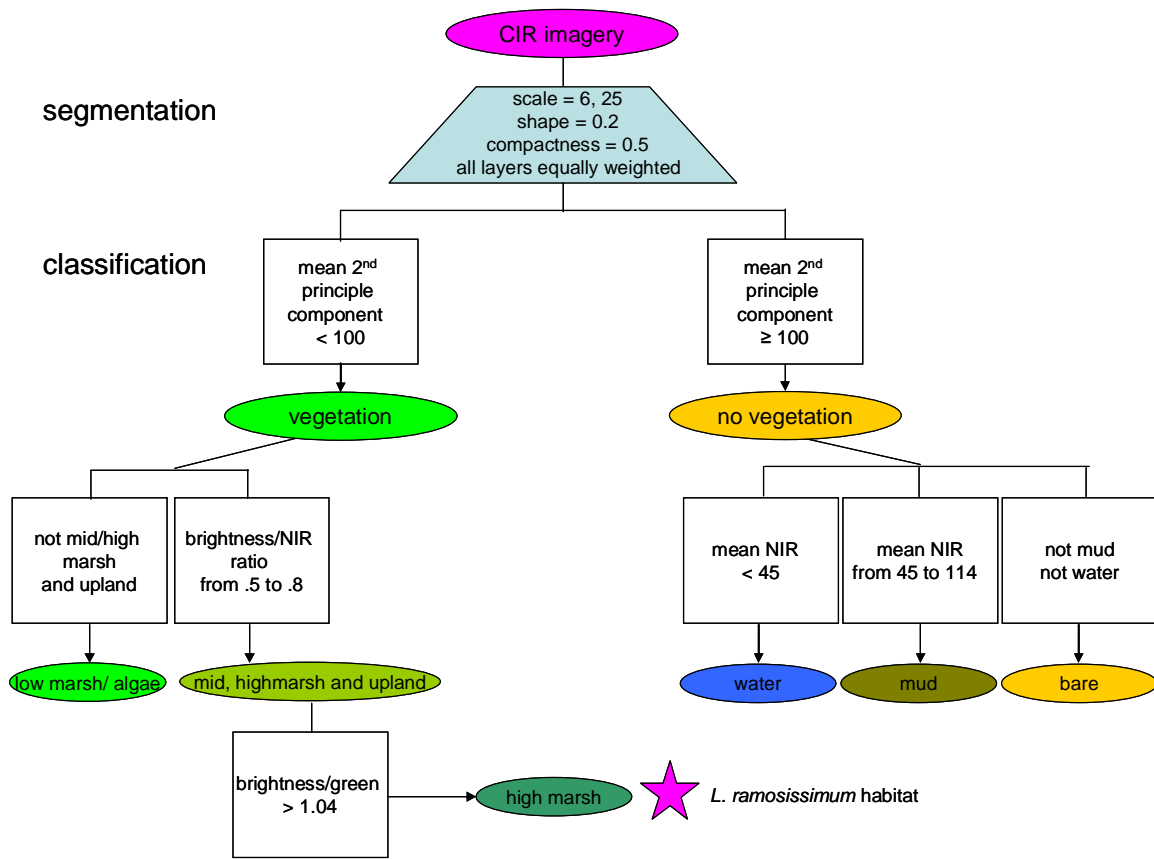


Figure 6: Rule set developed and executed in Definiens Developer to identify high marsh habitat and adjacent broad habitat classes using CIR aerial imagery. Rule set was run at two scales: 6 and 25.

Minimum Patch Size Detection

Rule sets were executed at two different spatial scales at both sites to test the importance of patch size on detection. *L. ramosissimum* patches range at both sites range from single plants less than 1 m² to patches about 600- 700 m² (Figure 7). During the initial segmentation step in Definiens, scale parameters were chosen so object sizes derived from both imagery sources would be comparable. Minimum objects sizes created in Definiens at the two scales are comparable to many small and medium *L. ramosissimum* patches at both sites (Table 2).

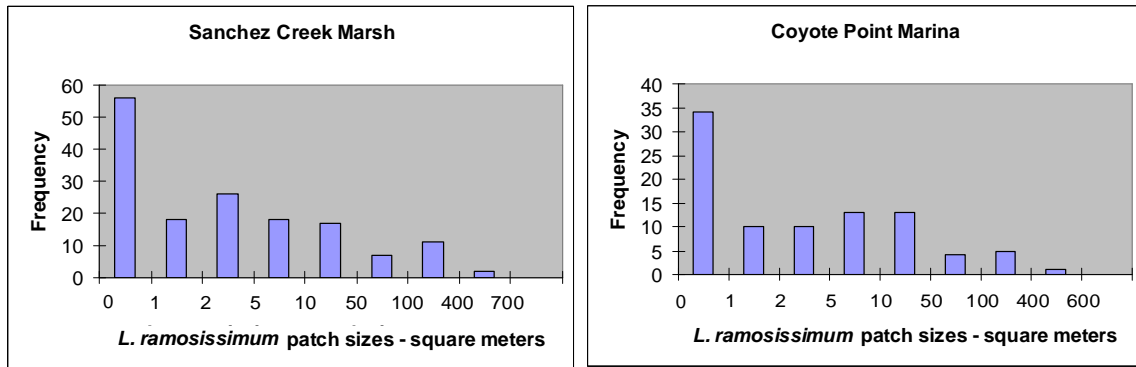


Figure 7: Distribution of *L. ramosissimum* patch sizes at both study sites. Histograms were generated from mapped *L. ramosissimum* polygons.

Table 2: To insure that image object sizes, and therefore minimum *L. ramosissimum* patch mapping sizes, were similar between imagery sources with different pixel sizes, different scale parameters were used for both imagery sources.

Imagery	Segmentation scale parameter	Average object size in square meters by location	
		Coyote Point Marina	Sanchez Creek Marsh
IKONOS 1 meter	scale 2 - small patch	1.8 m ²	1.9 m ²
	scale 10 – medium patch	42.7 m ²	46.8 m ²
CIR .33 meter	scale 6 - small patch	1.9 m ²	1.1 m ²
	scale 25 – medium patch	31.1 m ²	23.3 m ²

Use of Layers and Indices for Detection

Once high marsh and transitional upland habitats were the imagery layers were combined into a series of indices and ratios (Table 3, page 11) in Definiens and explored in a trial and error approach typical in OBIA to identify whether spectral properties of objects in *L. ramosissimum* patches could be used to separate the invader from other marsh and transitional upland species. This was accomplished using the Feature View in Definiens Developer (Figure 8, page 11). These visual comparisons were performed at both the small and medium patch spatial scales

Table 3: Layers, ratios, indices and other object features used to develop a rule set to detect *L. ramosissimum*. * Denotes features only tested on multispectral imagery.

Layers	Ratios	Indices	Object features
blue*	green/red	NDVI	hue
green	blue/green*	GNDVI	texture
red	blue/red*	blue/red index*	brightness
NIR	NIR/red	green/red index	distance from low marsh class
pc1	NIR/blue*		distance from upland class
pc2	NIR/green		standard deviations of layers,
pc3	brightness/NIR		ratios and indices
	brightness/red		
	brightness/green		
	brightness/blue*		
	blue/pc1*		
	red/pc1		
	green/pc1		
	nir/pc1		

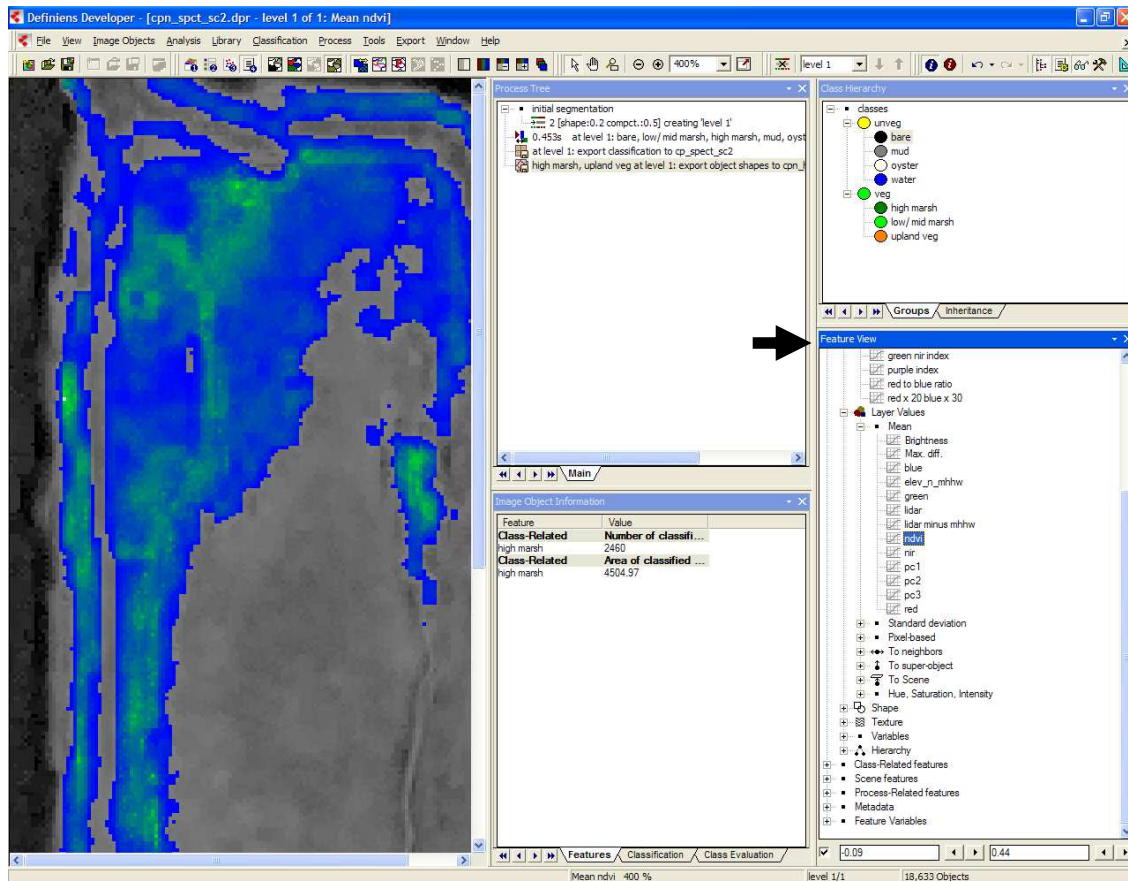


Figure 8: The Feature View in Definiens (arrow above) was used both to identify layer, ratio, and index values to classify broad habitat classes, and to try and parse *L. ramosissimum* from surrounding high marsh and upland transition habitat. In the screen shot above, objects with NDVI values between -.09 and .44 are selected in the map to the left.

Relationship between spectral values and patch characteristics

After spectral layers and indices were tested visually for their ability to detect *L. ramosissimum* in Definiens at different minimum patch sizes, the predictive power of indices and layer values relative to patch cover and percent flowering was explored. To do this, image objects with layer, ratio and index values were exported as shapefiles, spatially joined with mapped *L. ramosissimum* polygons in ArcGIS, then brought into Excel. Values were graphed as pairwise scatter plots and r^2 measured; with object values as dependent variables and patch flowering and cover as independent variables. This method has been used in previous studies to explore the predictive relationships between indices, ratios and species percent cover (Hunt, 2006).

These analyses were carried out using multispectral and CIR imagery at Sanchez Creek Marsh. Sanchez Creek Marsh was chosen for this analysis because Coyote Point Marina imagery had already been thoroughly explored during the Definiens rule set development.

Unsupervised classifications

Finally, a series of unsupervised pixel-based classifications were performed using Erdas Imagine to test whether ISODATA clustering might be useful for mapping the invader, and results checked against mapped polygons. To do this, the high marsh habitat class defined using Definiens in the northern half of Coyote Point was exported as a shapefile, converted to an Erdas AOI file and used to mask pixel-based analysis. Cluster analyses were run with 6 and 10 classes in high marsh habitat. ISODATA clustering analysis was also run on the unmasked Sanchez Creek Marsh image with 20 and 30 classes.

Results:

Study area ground-truthing:

Results of mapping *L. ramosissimum* percent cover and flowering at Coyote Point Marina and Sanchez Creek Marsh show the variety of patch sizes, cover and percent flowering present at the time of imagery acquisition (Figs 2.1 and 2.2, Appendix). Plotting patch size versus percent cover of patches indicates that while smaller patches have variable percent cover, larger patches regularly have greater than 50 percent cover (Figure 9), indicating both large and small patches with dense cover were present during image acquisition.

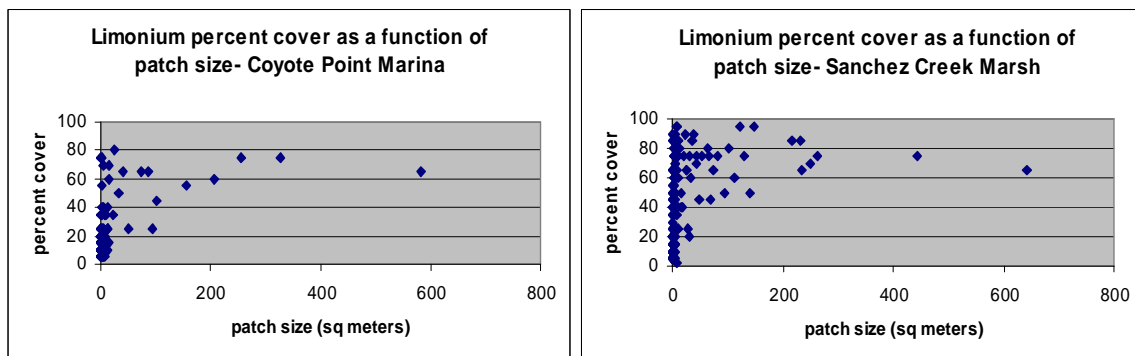


Figure 9: Large and small patches had high percent cover at both marshes during image acquisition.

Rule sets to identify broad habitat classes:

Definiens rule sets to classify broad habitat classes were successful in restricting *L. ramosissimum* polygons into high marsh and upland classes for focused analysis using both imagery types. However, the proportion of *L. ramosissimum* at ground truthed patch locations classified as high marsh, upland and bare habitat varied at different marshes, with the imagery, and at different scales (Table 4.1, Table 4.2). Classified maps of the northern section of Coyote Point Marina from both imagery sources relative to mapped *L. ramosissimum* patches are shown in Figure 10, page 14.

Table 4.1: For CIR imagery, at locations of ground mapped *L. ramosissimum* polygons percent of each habitat class assigned in Definiens by site and scale.

Color infrared (CIR) aerial imagery						
	Coyote Point Marina, northern half		Coyote Point Marina, southern half		Sanchez Creek Marsh	
	Scale 6	Scale 25	Scale 6	Scale 25	Scale 6	Scale 25
high marsh	57.7	66.3	38.2	36.9	20.2	28.4
upland	38.1	31.8	44.2	47.9	63.1	60.2
bare	1.7	0.9	16.3	14.7	3.5	3.8
low marsh	2.4	0.8	1.4	0.5	13.0	7.6
mud	0.2	0.1	0.0	0.0	0.1	0.0

Table 4.2: For multispectral imagery, at locations of ground mapped *L. ramosissimum* polygons, percent of each habitat class assigned in Definiens by site and scale.

Multispectral satellite imagery						
	Coyote Point Marina, northern half		Coyote Point Marina, southern half		Sanchez Creek Marsh	
	Scale 2	Scale 10	Scale 2	Scale 10	Scale 2	Scale 10
high marsh	80.2	88.2	35.9	48.4	57.8	64.9
upland	17.3	11.6	31.4	47.2	13.6	17.0
bare	0.0	0.0	31.4	0.6	13.6	0.1
low marsh	2.5	0.2	0.8	0.8	14.8	17.6
mud	0.0	0.1	0.5	0.0	0.2	0.4
oyster	0.0	0.0	0.2	0.0	0.1	0.0

Use of layers, ratios and indices for detection:

While rule sets were useful in isolating habitat invaded by *L. ramosissimum*, additional Feature View analysis using layer, ratio and index values within high marsh and upland habitat failed to identify value ranges that separated *L. ramosissimum* from surrounding habitats. Because this was carried out in an iterative, trial and error process within Definiens, these results at the broad habitat scale are not easily summarized. However, a list of key ratios and indices which were examined, and observations about their utility in classifying marsh habitats are included in Table 2, Appendix.

Relationship between spectral values and patch characteristics

Results of a series of pair wise correlations show no strong predictive relationships between patch percent cover and flowering existed for any of the layers, ratios or indices examined, regardless of imagery source. (Figures 3.1 and 3.2, Appendix).

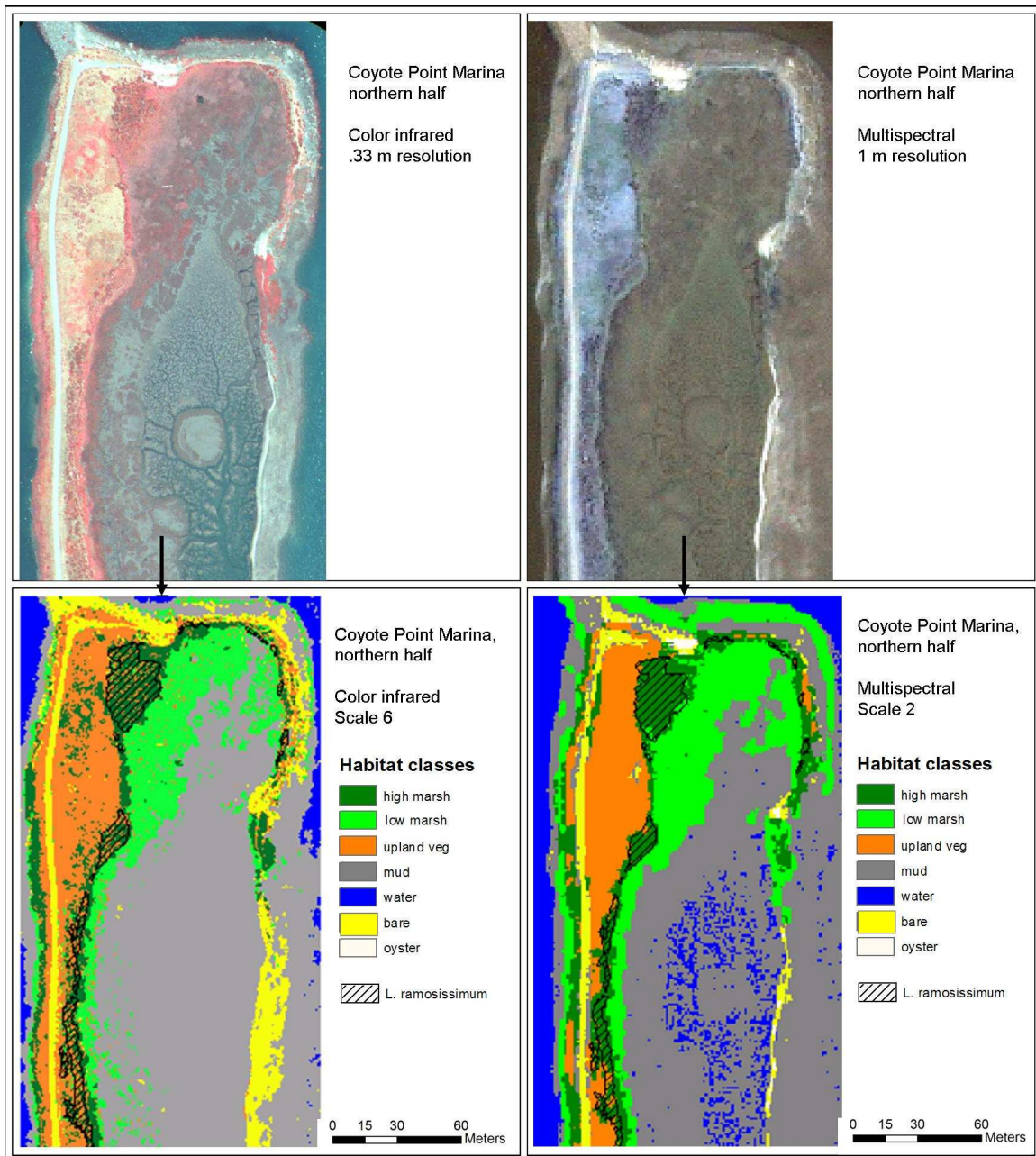


Figure 10: Raw imagery (top) and maps (bottom) classified using rule sets in Definiens of the Northern half of Coyote Point Marina. Maps show locations with *L. ramosissimum* displayed relative to broad habitat map results.

Unsupervised classification:

Unsupervised classifications performed using Erdas imagine with both imagery types appear to readily distinguish broad marsh habitat types. However, whether images were classified in their entirety (Figure 10, page 15), or whether cluster analysis was limited to masked high marsh habitat (Figure 11, page 16), significant spectral confusion between *L. ramosissimum* patches, marsh and upland habitats remained. Visual examination reveals no pixel classes are

located dominantly in ground mapped *L. ramosissimum* polygons. Pixel classes that regularly appear in *L. ramosissimum* polygons are wide spread in classes that correspond with dominant native high marsh species, upland vegetation, and bare ground.

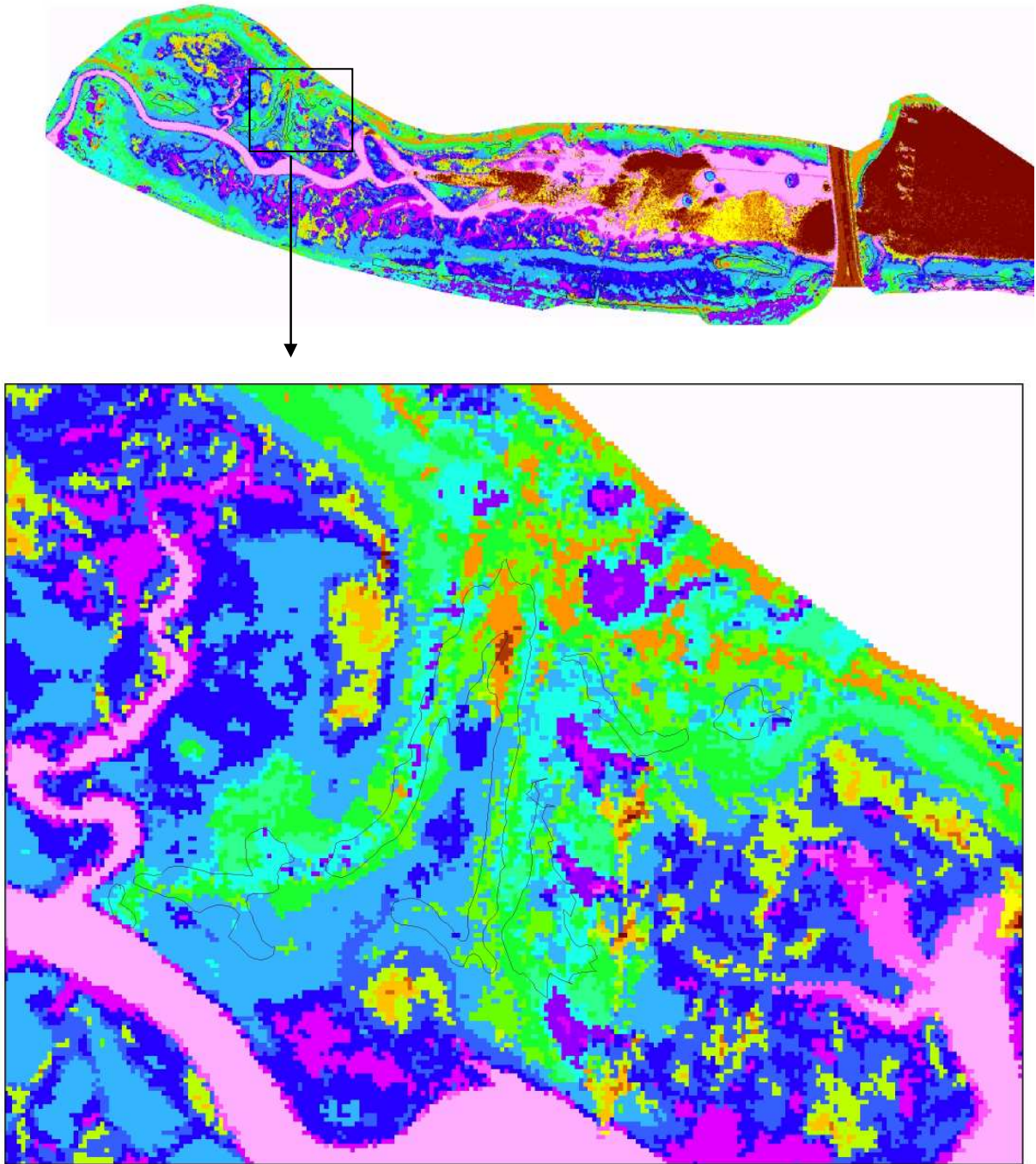


Figure 10: CIR imagery of Sanchez Creek Marsh clustered using an unsupervised classification into 20 habitat classes. Results show spectral confusion between *L. ramosissimum* (outlined above) and other high marsh and upland habitats.

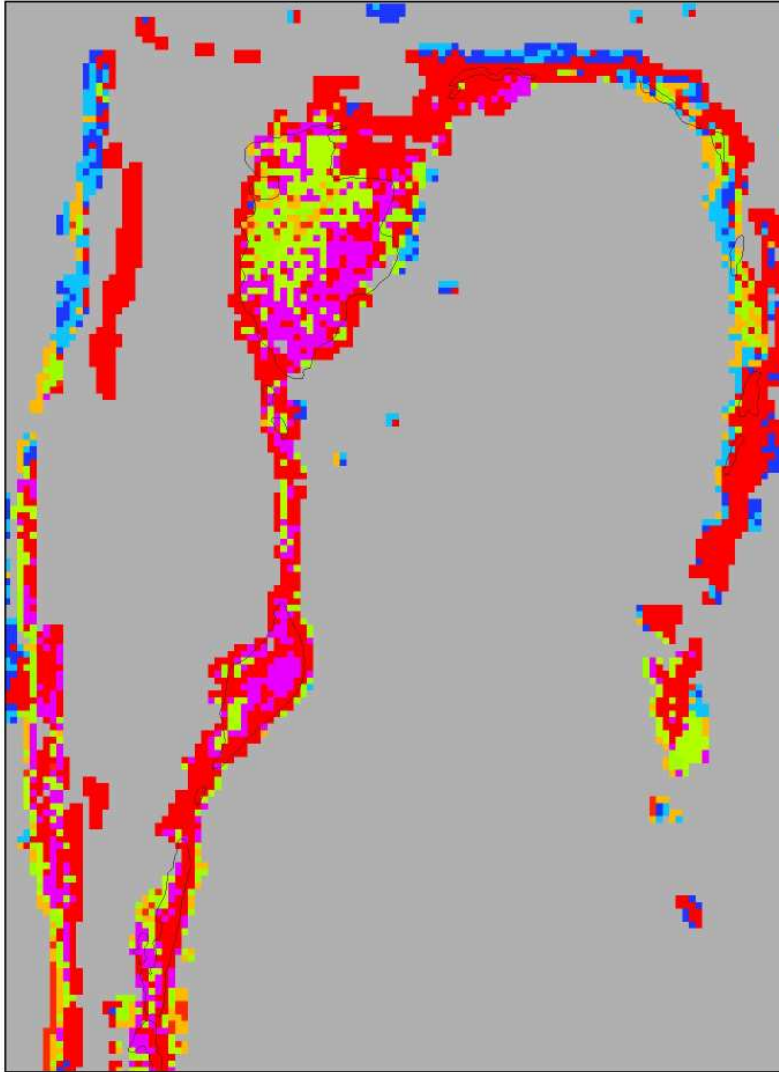


Figure 11: Multispectral imagery of Sanchez Creek Marsh clustered using an unsupervised classification into 8 habitat classes. Results show spectral confusion between *L. ramosissimum* (outlined above) and other high marsh habitats.

Discussion

No spectral characteristics were discovered to detect *L. ramosissimum* using high resolution CIR and multispectral sources, even though the imagery included patches in flower which were many times larger than the imagery resolution. This is likely because of the types of sensors used in relation to *L. ramosissimum*'s spectral characteristics, but could also be a function of the pixel segmentation and clustering algorithms used and methods applied. Further analysis with these images, archived imagery, and field studies would help to determine which the case is, and whether a remote sensing detection protocol may yet be developed for *L. ramosissimum*.

It is clear from the Feature View analysis in Definiens and the pairwise testing for predictive relationships between patch characteristics and spectral layers, ratios and indices and, that no

obvious spectral features readily distinguish *L. ramosissimum* from surrounding vegetation using CIR and IKONOS multispectral imagery.

In the case of IKONOS imagery, this may be because purple, the visually dominant color of flowering *L. ramosissimum*, occurs in the 400- 410 nm range of the spectrum and IKONOS imagery only detects wavelengths of light longer than 455 nm. Also, blue light is the wavelength most scattered by the earth's atmosphere, reducing detection potential of these flowers with satellite imagery. Additionally, the color and near infrared bands in IKONOS imagery are collected at 4 meter resolution, then pan-sharpened to 1meter. In this process, nearby, non- *L. ramosissimum* species are spectrally averaged into pixels where *L. ramosissimum* is present. This spectral dilution of pixels is likely exacerbated by the narrow, linear zonation of *L. ramosissimum* at some locations in the marshes studied.

In the case of CIR aerial imagery, which suffers from far less atmospheric scattering and which has considerably higher original pixel resolution at color and near infrared wavelengths than IKONOS, there is no collection of blue light. This is likely why no flower based spectral signature was apparent with the CIR imagery. *L. ramosissimum*'s vegetative growth form, on the other hand, which consists of perennial, green basal rosettes, likely contributes strongly to pixel spectra, especially when densely growing. However, the densest *L. ramosissimum* patches were confused with other high marsh species, indicating the spectral signature appears too similar to other plant species for ready detection.

Both Definiens and Erdas pixel clustering algorithms alternatively grouped *L. ramosissimum* with upland and high marsh species when patch percent cover was low, yet readily distinguished between upland and high marsh vegetation. One explanation of this may be that reflectance in low percent cover patches in upland transition areas are dominated by background upland vegetation and soil moisture differences, rather than the "high marsh" signature of dense *L. ramosissimum* patches. Dense patches of *L. ramosissimum* were regularly classified with high marsh species in both Definiens and Erdas.

Methods used for clustering pixels and classifying images may also contribute to the failure to detect *L. ramosissimum*. Hunt and Williams, 2006 concluded their inability to detect leafy spurge with multispectral satellite imagery versus hyperspectral imagery was not the result of insufficient sensor range or the spectral resolution of multispectral imagery, but rather the difference between classification algorithms available for hyperspectral and multispectral imagery. The OBIA approach used in this study focused on developing a rule set using relatively simple, univariate spectral properties for detection. It's possible more sophisticated classification procedures could help resolve *L. ramosissimum*.

More sophisticated classification tools exist within Definiens- such as the nearest neighbor (NN) approach, in which object features and samples of each class of interest are selected by the user and all image objects are assigned to the closest class in a multivariate space. This approach is possible with the existing imagery, though more thorough ground truthing would be required to accurately assign samples to classes. Also, object features chosen must be predictive of *L. ramosissimum* and from correlation analysis, this appears unlikely.

Object features could also be exported as they were in this study, and then analyzed with a multivariate statistical analysis, allowing both degree of flowering and percent cover to be

compared simultaneously with multiple spectral features. Similarly, in Erdas, while an unsupervised classification approach is useful to test for obvious spectral differences between species, this process can certainly be refined using a supervised classification approach, which may yield more accurate mapping results.

Though additional analysis options exist with the current imagery, the fact that no clear spectral signature is readily available makes the possibility of landscape scale detection unlikely with either of the imagery sources used in this study. Refining methods to detect subtle distinctions in the images used in may improve mapping results with the existing imagery, but the lack of an obvious spectral signature for *L. ramosissimum* makes the development of an efficient landscape scale detection protocol using either CIR or IKONOS imagery sources unlikely.

Hyperspectral aerial imagery may more readily detect *L. ramosissimum*, because of increased spectral range and resolution. Hyperspectral sensors collect spectra starting around 400nm, which would detect violet light, particularly if the sensor is aerially deployed (vs. satellite). Archived hyperspectral imagery may exist for the Sanchez Creek Marsh, Coyote Point Marina, or other *L. ramosissimum* locations that could be tested for detection potential at low cost.

The potential for hyperspectral sensor detection of *L. ramosissimum* could also be evaluated by field studies using a hand-held field spectrometer (ie the GER 1500 collects spectra from 350 nm-1050 nm). A study evaluating the spectral differences between *L. ramosissimum* and surrounding marsh and transitional upland vegetation at different times of the year would determine when phenological differences between species will maximize detection. During the fall and winter, some native march vegetation senesce, but *L. ramosissimum* remains green year round. This may present an opportunity for mapping.

Early detection and rapid response is critical for cost-effective management of invasive plant species. Remote sensing is a useful tool to aid in detection, but the ability and scale at which a given species can be detected varies with the imagery used and the spectral context of the plant. A systematic study of which invasive species can be detected by which imagery source(s) and how detection rates vary seasonally is recommended as a key step towards developing a remote sensing-based invasive species monitoring program.

References:

Archbald, G. and K. Boyer. Evaluating the Potential for Spread of an Invasive Forb, *Limonium ramosissimum ssp provinciale* in San Francisco Bay Salt Marshes, 2010. Oral Presentation, San Francisco Bay Estuary Conference.

Andrew, M. E and S. L. Ustin. 2008. The role of environmental context in mapping invasive plants with hyperspectral image data. *Remote Sensing of Environment* 112:4301–4317.

Bay Area Early Detection Network, 2010. Priority Species List. Accessed at www.baedn.org, November, 2010

Belluco, E., Camuffo, M., Ferrari, S., Modenese, L., Silvestri, S., Marani, A., and M. Marani. 2006. Mapping salt-marsh vegetation by multispectral and hyperspectral remote sensing. *Remote Sensing of the Environment*. 105: 54-67.

Blesius, Leonhard, *San Francisco State University*, personal communication. October, 2010.

Cuneo, P., Jacobson, C.R. and M. R. Leishman, 2009. Landscape-scale detection and mapping of invasive African Olive (*Olea europaea* L. *ssp. cuspidata*) in SW Sydney, Australia using satellite remote sensing. *Applied Vegetation Science* 12: 145–154, 2009

Everitt, J. H., Escobar, D. E., Alaniz, M. A., Davis, M. R. and J. V. Richerson. 1996. Using spatial information technologies to map Chinese tamarisk (*Tamarix chinensis*) infestations. *Weed Science*. 44:194–201.

Foxgrover, A. C., and B. E. Jaffe, 2005. South San Francisco Bay 2004 Topographic Lidar Survey: Data Overview and Preliminary Quality Assessment. U.S. Geological Survey Pacific Science Center, Santa Cruz, CA. Open-File Report 2005–1284.

Fulfroost, Brian, *Design Community and Environment*. Personal communication, November, 2010.

Grossinger, R., Alexander, J., Cohen, A. N., and J. N. Collins, 1998. Introduced tidal marsh plants in the San Francisco Estuary regional distribution and priorities for control. *San Francisco Estuary Institute*, Richmond, CA 94804.

Hunt, R. E., Parker Williams, A. E., 2006. Detection of Flowering Leafy Spurge With Satellite Multispectral Imagery. *Rangeland Ecol Manage* 59:494–499

Hunt, R., Hamilton, R., and J. Everitt, 2010. What weeds can be remotely sensed? A weed managers guide to remote sensing and GIS – Mapping & monitoring. *USDA Forest Service Remote Sensing Applications Center*, Salt Lake City, UT.

Hogle, Ingrid, *Invasive Spartina Project*. Personal Communication. December, 2010.

Lass, L. W., Prather, T.S., Glenn, K. F., Weber, K.T. and T. M. Jacob, 2005. A review of remote sensing of invasive weeds and example of the early detection of spotted knapweed (*Centaurea maculosa*) and babysbreath (*Gypsophila paniculata*) with a hyperspectral sensor. *Weed Science*, 53(2):242-251. 2005.

Lawes, R.A. & Wallace, J.F. 2006. Using temporal sequences of Landsat imagery to detect trends in *Acacia nilotica* in the Mitchell Grass plains. In: Preston, C., Watts, J.H. & Crossman, N.D. (eds.) Proceedings of the fifteenth Australian Weeds Conference. pp. 474–476. *Weed Management Society of South Australia Inc.*, Adelaide.

Lass, L. W. and T. S. Prather. 2004. Detecting the locations of Brazilian pepper trees in the Everglades with a hyperspectral sensor. *Weed Technology*. 18:437–442.

Margaret E. Andrew, Susan L. Ustin (2006) Spectral and physiological uniqueness of perennial pepperweed (*Lepidium latifolium*). *Weed Science*, 54:6, 1051-1062.

Rosso, P.H., S.L. Ustin, A. Hastings. 2005. Mapping marshland vegetation of San Francisco Bay, California, using hyperspectral data. *International Journal of Remote Sensing*, 26(23):5169–5191.

Tuxen, K. and M. Kelly. 2009. Object-Based Image Analysis, Chpt 4: Multi-scale functional mapping of tidal marsh vegetation using object-based image analysis. *Springer Berlin Heidelberg*, 1863-2246.

Westbrooks, R. G., 2004. New Approaches for Early Detection and Rapid Response to Invasive Plants in the United States. *Weed Technology*, 18:1468-1471.

Appendix:

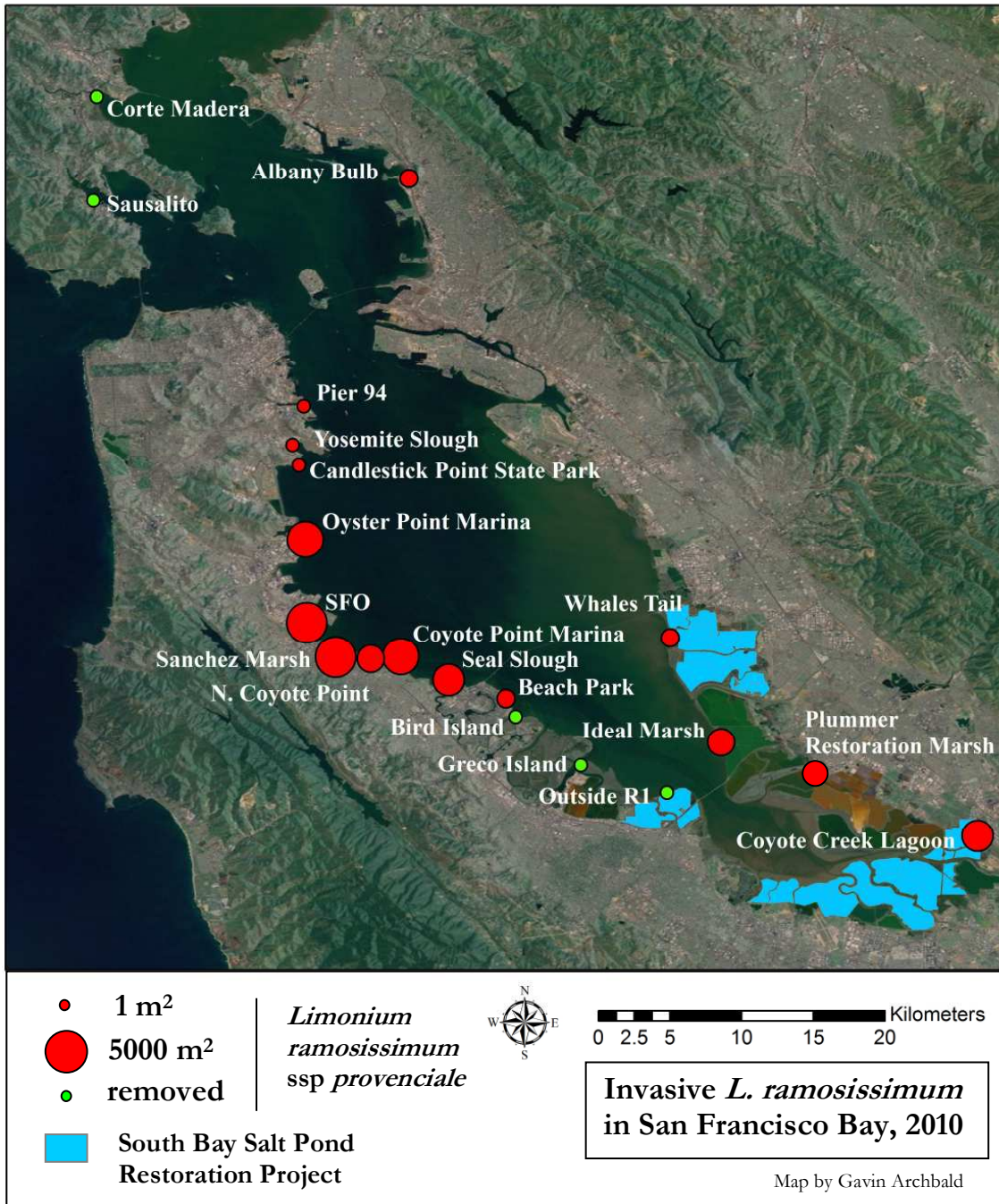


Figure 1: Known locations of *L. ramosissimum* ssp. *provinciale* in San Francisco Bay.

Table 1: *L. ramosissimum* population sizes in San Francisco Bay. Highlighted locations were used for image analysis.

Location	Area (m ²)
Sanchez Marsh	4361
SFO	3859
Coyote Point Marina	2300
Oyster Point Marina	1592
Coyote Creek Lagoon	1117
Seal Slough	519
N. Coyote Point	449
Ideal Marsh	239
Whales Tail	36
Albany Bulb	32
Beach Park	13
Yosemite Slough	2
Outside R1	2
Sausalito	1
Corte Madera	1
Candlestick Point State Park	1
Pier 94	1
Bird Island	1
Greco Island	1
Plummer Restoration Marsh	unknown

Table 2: Key layers, ratios and indices used in an effort to detect *L. ramosissimum* and comments on their observed general utility.

<u>Index</u>	<u>Utility in distinguishing:</u>
NDVI Normalized Difference Vegetative Index = (NIR – red) / (NIR + red)	Vegetation from bare ground
GNDVI = (NIR – green) / (NIR + green)	Vegetation from bare ground
G/R ratio = green / red	Upland veg., but noisy
NDVI and mean green layer	Algae on mudflats from <i>Spartina</i>
NIR	Water from mud and vegetation
Standard deviation of layer	Pure from mixed vegetation patches
Hue (red, green blue)	Finds <i>Grenselia stricta</i>
Blue/Red index = (blue – red) / (blue + red)	Identifies marsh zones w/ IKONOS
Blue/Green index = (blue – green) / (blue + green)	Separates terrestrial dirt from mud
Brightness/ NIR	Particularly useful for CIR imagery
Brightness/ green	Particularly useful for CIR imagery

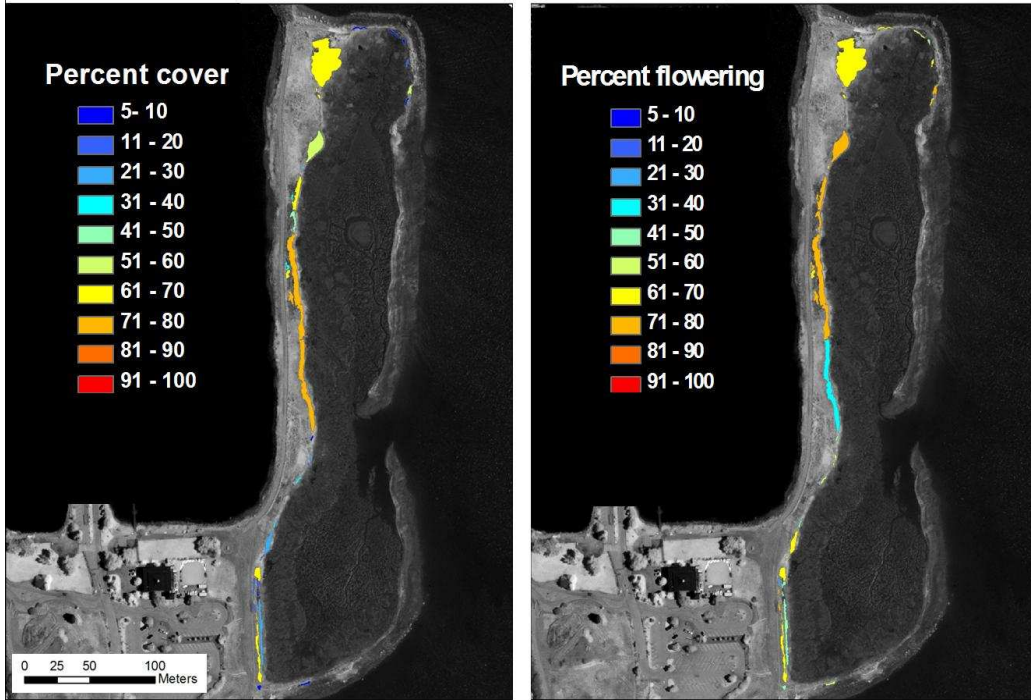


Figure 2.1: Percent cover and flowering at Coyote Point Marina on 7/8/2010.

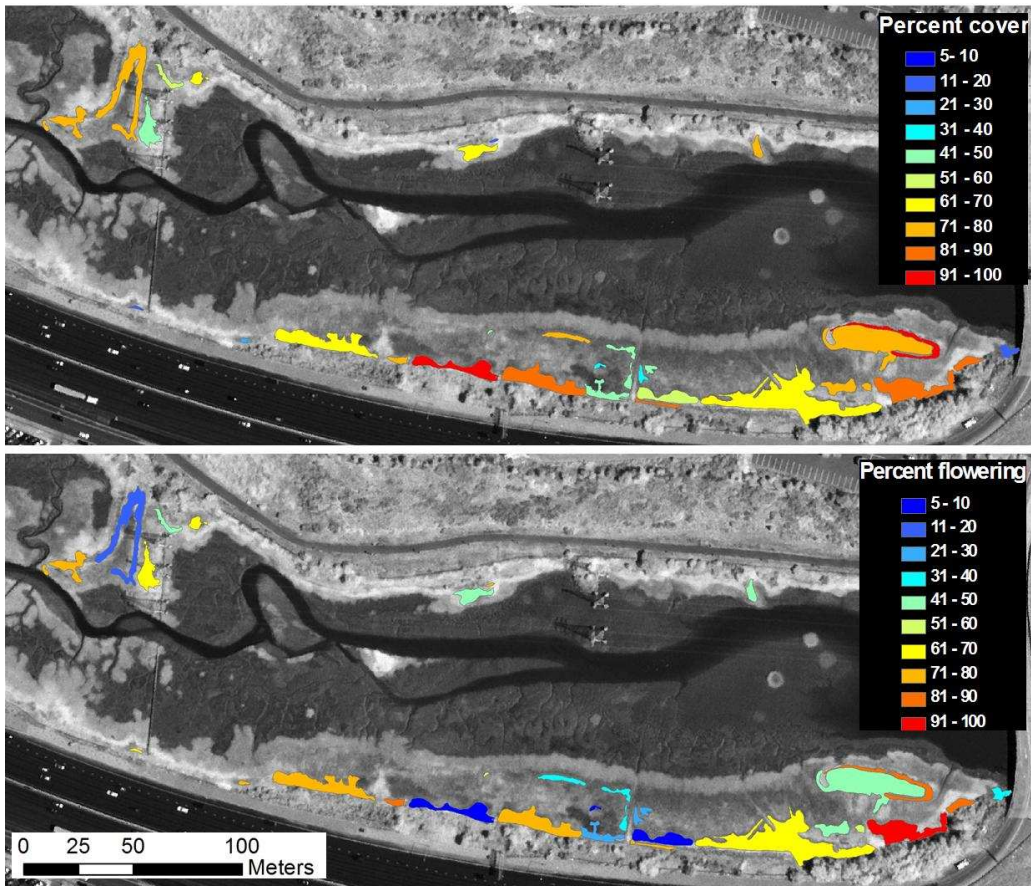


Figure 2.2: Percent cover and flowering at Sanchez Creek Marsh on 7/8/2010.

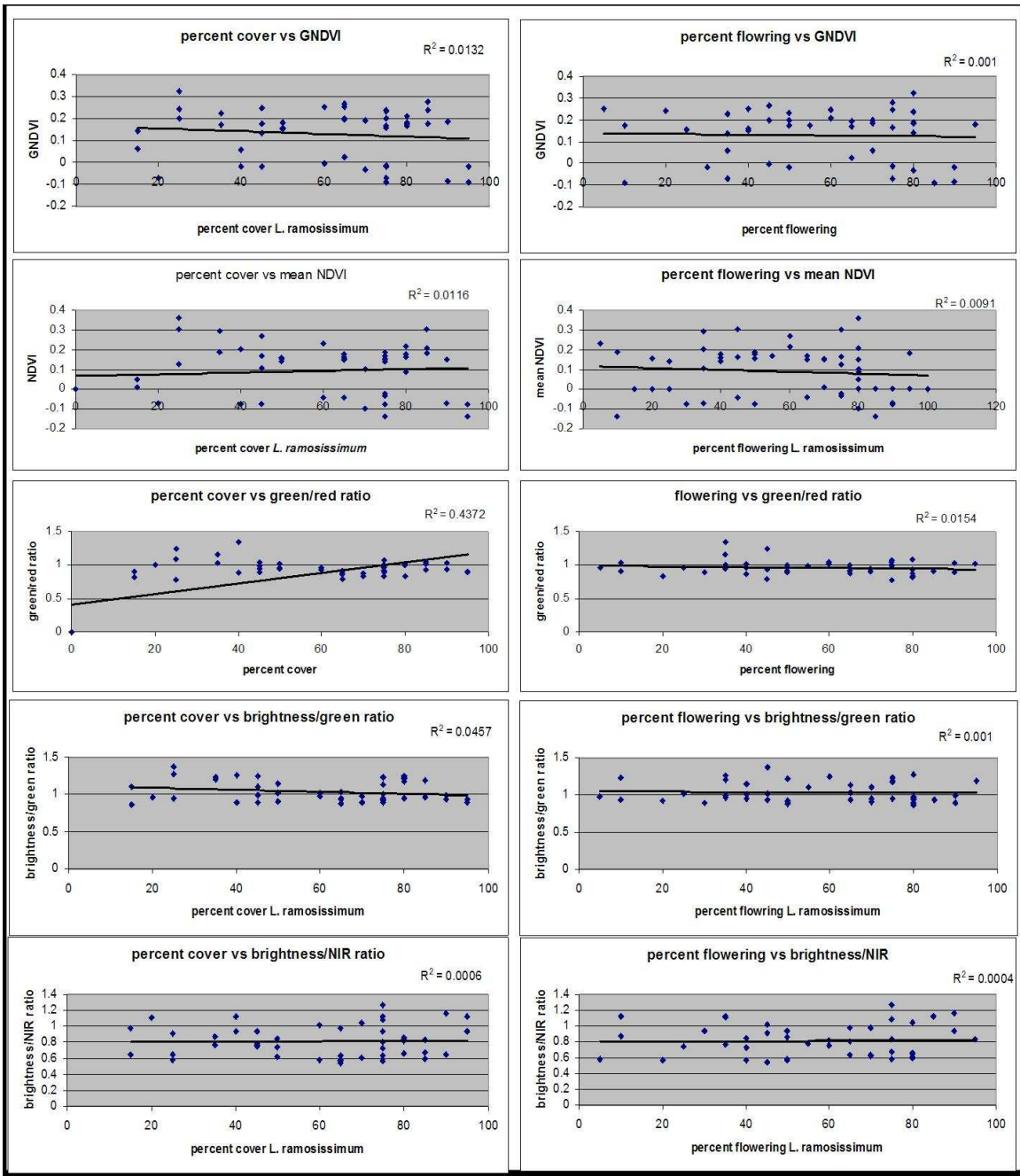


Figure 3.1: No significant predictive relationships were found between a *L. ramosissimum* percent cover and flowering vs a series of vegetation indices and ratios derived from CIR imagery at Sanchez Creek Marsh.

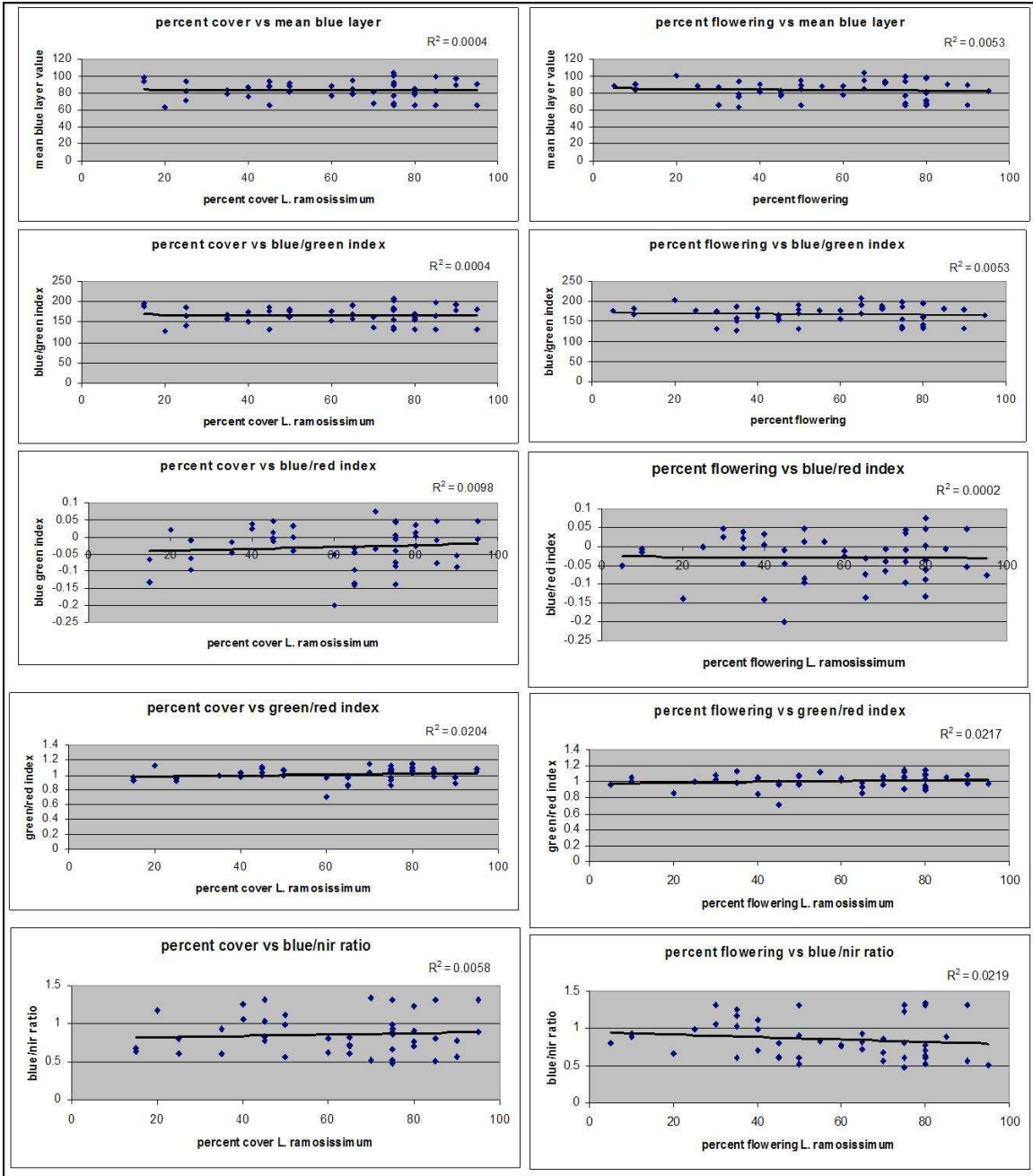


Figure 3.2: No significant predictive relationships were found between *L. ramosissimum* percent cover and flowering vs a series of layers, ratios and indices derived from IKONOS imagery at Sanchez Creek Marsh..